

Line shape parameters study of the $6p7p$ (1P_1 , 3D_1 and 3P_1): Autoionizing resonances in barium

M.A. Kalyar, S. Mahmood, S.-U. Haq, N. Amin, and M.A. Baig^a

Atomic and Molecular Physics Laboratory, Department of Physics, Quaid-i-Azam University, Islamabad 45320, Pakistan

Received 29 July 2006 / Received in final form 2 October 2006

Published online 20 October 2006 – © EDP Sciences, Società Italiana di Fisica, Springer-Verlag 2006

Abstract. We report a systematic line shape analysis study of the $6p7p$ configuration based 1P_1 , 3D_1 and 3P_1 autoionizing resonances in barium using a Nd:YAG pumped dye laser system in conjunction with a thermionic diode ion detector. The even parity isolated autoionizing resonances have been approached via four intermediate states $6snp$ 1P_1 ($6 \leq n \leq 8$) and $5d6p$ 1P_1 . A comparison of the Fano parameters of the resonance profiles reveals that the width of an autoionizing resonance is independent of the excitation path while the line profile parameter changes with the selection of different intermediate states.

PACS. 32.30.Jc Visible and ultraviolet spectra – 32.70.Jz Line shapes, widths, and shifts – 32.80.Dz Autoionization – 32.80.Fb Photoionization of atoms and ions

1 Introduction

The energy positions of the Rydberg states and autoionizing resonances have been extensively studied since the advent of narrow bandwidth tunable dye lasers and results have been discussed in a number of books [1–5]. Alkaline earth metals are low-density metals with two valence electrons. These elements exhibit interesting phenomenon of autoionization occurring above the first ionization threshold that results from simultaneous excitation of both the valence ns electrons. Autoionizing resonances are the atomic states that emerge due to configuration mixing of the discrete excited states with the continuum channels. As a result the lifetime of the discrete states decreases, the lines get broadened and also show asymmetric profiles. The profile of an autoionizing line depends upon the path through which it is excited. Ganz et al. [6] pioneered the line profile dependence on the excitation path in the study of the Ne ($14s'$, $J = 1$) autoionizing resonances acquired from different intermediate states ($2p^53p$, $J = 1, 2$). It was inferred that the shape of the resonance varies with the change of the intermediate state whereas the resonance width remains constant. Keller et al. [7] investigated the line shape dependence of the autoionizing resonances of barium on the excitation path. A significant difference in the profiles of the autoionizing lines was observed for the excitation path involving different intermediate states. It was reported that the angular distribution of the photoelectrons collected across the range of the autoionizing resonances show strong variations as well as the spin-orbit interactions. Baig et al. [8] studied the line shape of the $(4d^2 + 5p^2)^1D_2$ even parity isolated autoion-

izing resonance of strontium approached directly from the ground state by two-photon excitation and via two-step excitation process using the $5s5p$ 1P_1 as an intermediate state. The line shape parameters were extracted by fitting the two-channel modal of Multi-channel Quantum Defect Theory (MQDT) to the observed data and it was inferred that the width of the resonance remains the same while the line shape parameter differs for the two processes. Stellpflug et al. [9] examined the $5p^5(^2P_{1/2})20s'[1/2]_1$ and $5p^5(^2P_{1/2})18d'[3/2]_1$ autoionizing resonances in xenon approached via $5p^5(^2P_{1/2})6p'[1/2]_0$ and $5p^5(^2P_{3/2})6p[1/2]_0$ intermediate states. The photoelectron spectra of the autoionizing states was obtained by varying the frequency of the single-photon ionizing laser while the exciting laser pulse was tuned to the two-photon resonance between the ground state and the intermediate state. It was observed that the line width Γ of the autoionizing resonances remains constant whereas significant changes were observed in the line profile parameter q corresponding to two different intermediate levels. The line shapes of the autoionization resonances were also analyzed theoretically using Pauli-Fock approximation including core polarization [9].

The autoionizing spectra of barium have been studied extensively ([10–14] and references therein) but comparatively little information is available about the line shape dependence of the autoionizing resonances on the excitation channels. Camus et al. [15] observed broad resonances above the $5d$ threshold corresponding to the $6p7p$ configuration by two-step optogalvonic spectroscopy and compared their results with the calculated energies using Slater-Condon calculations. Elizarov and Cherepkov [16] developed a method for the experimental measurements of the total angular momentum of the autoionizing states

^a e-mail: baig@qau.edu.pk

by two-photon polarization spectroscopy and successfully applied to designate the $6p7p$ configuration based autoionizing states of Ba. Bobashev et al. [17] employed the two-step laser excitation to study the profiles of these autoionizing resonances with a time of flight mass spectrometer and measured the widths and the line profile parameter ‘ q ’ using the Fano Formula [18]. Luc-Koenig et al. [19] theoretically investigated the asymmetrical photoionization spectra of the $6p7p$ autoionizing resonances from the $6s6p$ 1P_1 and $6s7p$ 1P_1 intermediate states using the R -matrix and Multi-channel Quantum Defect Theory calculations. The energy positions and widths of the $6p7p$ autoionizing resonances were calculated from the $6s7p$ 1P_1 intermediate state, with and without the dielectric core polarization correction term.

The motivation of the present studies was to extract the line profile index parameter ‘ q ’ for different intermediate states. These intermediate states were selected so that every time the intermediate state is changed, the principal quantum number increases i.e. $6s6p$, $6s7p$ and $6s8p$ respectively. Consequently, the difference between the line shapes of the corresponding autoionizing lines will reflect the contribution of an additional node in the wave function of the intermediate state. In this paper, we present new studies on the effect of different excitation pathways on the line profiles of the $6p7p$ configuration based 1P_1 , 3D_1 and 3P_1 autoionizing resonances of barium by tuning the first exciting laser to four intermediate states $6snp$ 1P_1 ($6 \leq n \leq 8$) and $5d6p$ 1P_1 and by scanning the second laser to approach the autoionizing resonances. We have observed a significant change in the line shape of the autoionizing resonances based on the $6p7p$ configuration by changing the excitation path via different intermediate states while there seems to be no change in the line width of the resonances.

2 Experimental set-up

The experimental arrangements to study the $6p7p$ autoionizing resonances of barium are the same as described in our earlier work [8, 20, 21]. It consists of a Nd:YAG laser, a thermionic diode ion detector and a commercially available hollow cathode lamp. The laser system comprised of a Q-switched Nd:YAG laser (Quanta-Ray GCR-11); 10 Hz repetition rate, pulse duration ≈ 5 –7 ns, line width ≤ 0.3 cm^{-1} , equipped with KDP crystals for SHG (532 nm), THG (355 nm) and a wavelength separation assembly. Two home made Hanna type [22] dye lasers were pumped synchronously with the Nd:YAG laser. The cavity was formed between a flat mirror and a 2400 lines/mm holographic grating and the wavelength tuning was achieved by rotating the grating by a computer controlled stepper motor. The thermionic diode was composed of a stainless steel tube 52 cm long, 3.5 cm in diameter and 1 mm wall thickness. Both ends of the detector were water-cooled and sealed with 25 mm diameter quartz windows to transmit the laser beam. About 20 cm of the central part of the tube was heated by a clamp-shell oven operating at ≈ 930 K that corresponds to about 0.02 Torr

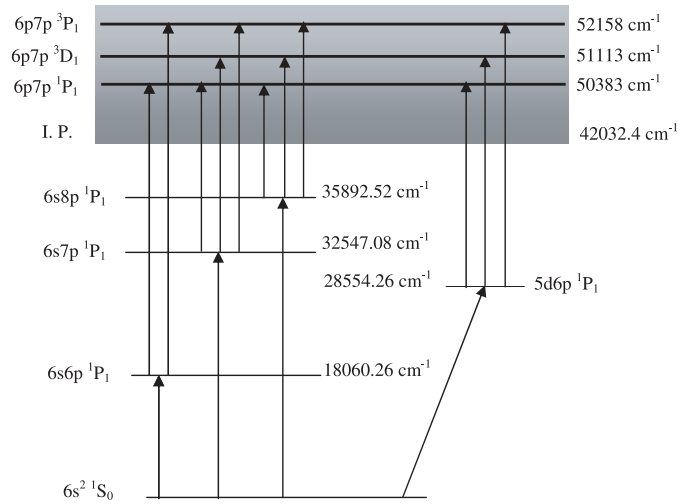


Fig. 1. Schematic diagram of the excitation scheme showing the intermediate levels and the three autoionizing resonances approached via different intermediate levels.

barium vapor pressure. Argon gas at a pressure of ≈ 1 Torr was used as a buffer gas that provided a uniform column of the barium vapors and prevented the contamination of quartz windows. The temperature was monitored by a Ni-Cr-Ni thermocouple and was maintained within $\pm 2\%$ by a temperature controller. A molybdenum wire 0.25 mm in diameter stretched axially, heated by a separate regulated DC power supply, served as a cathode for the ion detection.

The ionization signal was optimized by adjusting the pressure of the buffer gas and the cathode current. The scanning laser was divided into three parts and the main part was passed through the thermionic diode. A small fraction $\approx 10\%$ of the scanning laser was injected into a neon or argon filled hollow cathode lamp and the third part $\approx 10\%$ into a photodiode through a 2 mm thick solid fused silica Fabry-Perot etalon. The optogalvanic signal from the hollow cathode lamp was used for the absolute wavelength standard references and the etalon fringes served as the relative energy markers for analyses. The ion signal was taken across a 10 k Ω resistor through a 0.01 μF blocking capacitor and was registered on a 100 MHz storage oscilloscope. The three signals were simultaneously recorded on a computer using GPIB interface through three boxcar averagers (SRS 250) for subsequent analysis.

3 Results and discussion

Barium is the fifth element of the alkaline earth metals group possessing $6s^2$ 1S_0 ground state configuration. From the ground state, by single-photon absorption not only the $6snp$ ($J = 1$, odd parity) states can be excited but also the $5dnp$ ($J = 1$, odd parity) states can be approached due to the mixing between $6s^2$ and $5d^2$ configurations. We present a systematic study of the line profiles of the well-separated autoionizing resonances based on the $6p7p$ configuration of barium approached from the $6snp$

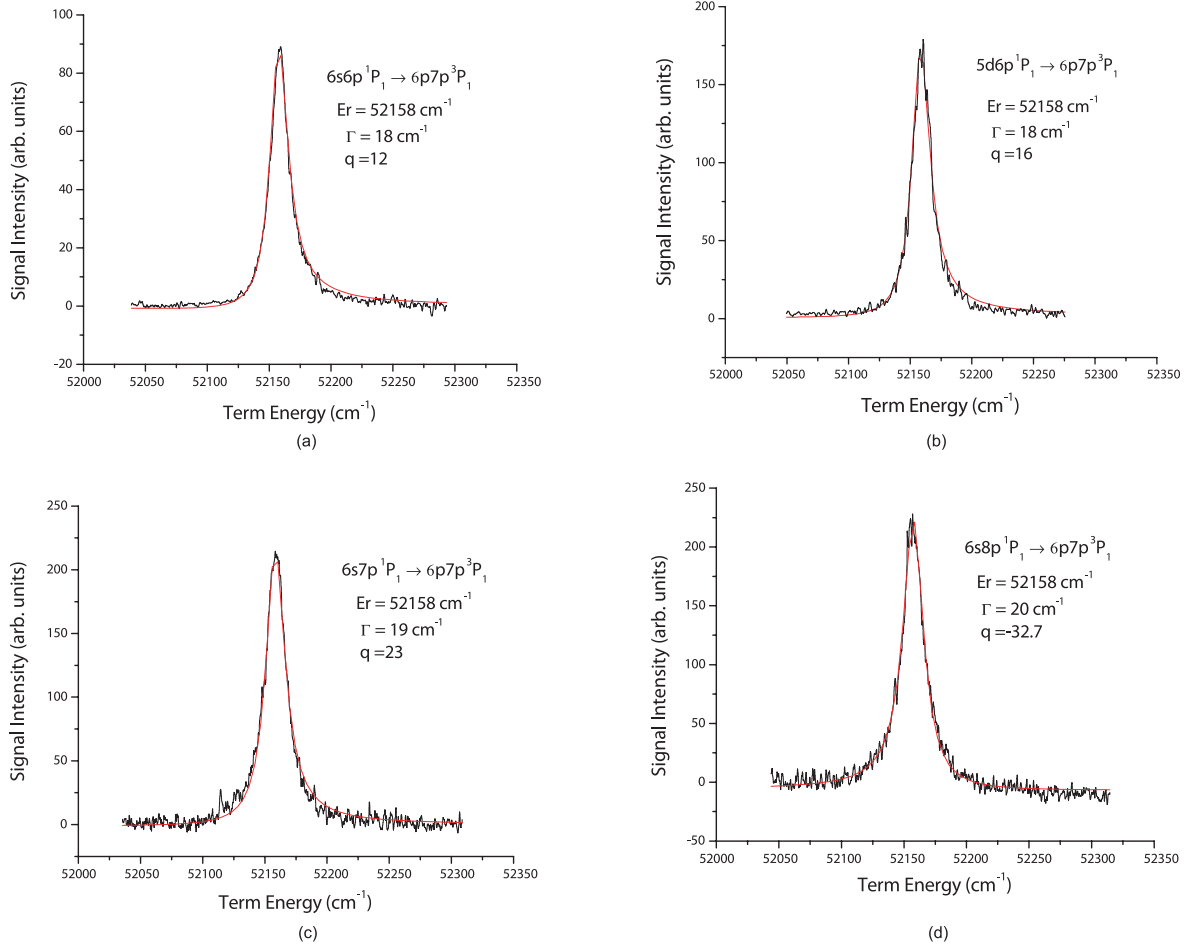
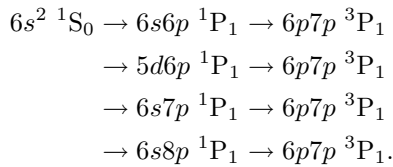


Fig. 2. The line shapes of the $6p7p\ ^3P_1$ autoionizing resonance of barium excited from (a) $6s6p\ ^1P_1$, (b) $5d6p\ ^1P_1$, (c) $6s7p\ ^1P_1$, (d) $6s8p\ ^1P_1$ the intermediate states. The smooth line is the Butler-Fano profile fitted to the experimental data.

1P_1 ($n = 6, 7, 8$) and $5d6p\ ^1P_1$ intermediate states. A schematic energy level diagram for the excitation is shown in Figure 1. The energy positions and assignment to the autoionizing resonances in LS coupling are taken from Camus et al. [15] whereas the energies of the intermediate states and ionization potential are taken from the NBS Tables [23].

In the first series of experiments, we have studied the line profile of the $6p7p\ ^3P_1$ autoionizing resonance corresponding to the following transitions



The atoms were resonantly excited to the $6s6p\ ^1P_1$ intermediate state by the dye laser charged with the Fluorescein-548 dye dissolved in methanol with a little amount of NaOH and pumped by the SHG (532 nm) of a Nd:YAG laser. In the second step, these excited atoms were promoted to the $6p7p\ ^3P_1$ autoionizing resonance using the dye laser charged with Rhodamine-610 dye and

pumped by the same Nd:YAG laser. The output of the second laser was frequency doubled by a BBO crystal to cover the scanning region from the 33940 cm^{-1} to 34290 cm^{-1} and the corresponding term energy from the 52000 cm^{-1} to 52350 cm^{-1} . Both the laser beams were spatially and temporally overlapped throughout the interaction region.

The line shape of the $6p7p\ ^3P_1$ autoionizing resonance approached from the $6s6p\ ^1P_1$ intermediate state is shown in Figure 2a, which is evidently asymmetric and broad. We have obtained the resonance energy, width and the line profile index parameter using the celebrated Fano relation [18] for an isolated autoionizing resonance:

$$\sigma(\varepsilon) = \sigma_a \frac{(q + \varepsilon)^2}{1 + \varepsilon^2} + \sigma_b \quad (1)$$

where $\varepsilon = [E - E_r]/(\Gamma/2)$ measures the departure of the incident photon energy E from the resonance energy E_r and $\Gamma = 2\pi|V_E|^2$ is the width of the autoionizing resonance, V_E gives the interaction between the discrete state and the continuum states. $\sigma(\varepsilon)$ represents the absorption cross section for photons of energy E , whereas σ_a and σ_b are the portions of the cross section of the continuum which interacts and does not interact with the discrete

Table 1. Butler-Fano profile parameters of $6p7p\ ^1P_1$, 3D_1 and 3P_1 autoionizing resonances.

Autoionizing resonance	Present work				Camus et al. [15] Exp.		Bobashev et al. [17] Exp.		Luc-Koenig et al. [19] Theory	
	Intermediate state	E_r (cm ⁻¹)	Γ (cm ⁻¹)	q	E_r (cm ⁻¹)	Γ (cm ⁻¹)	Γ (cm ⁻¹)	q	E_r (cm ⁻¹)	Γ (cm ⁻¹)
$6p7p\ ^3P_1$	$6s6p\ ^1P_1$	52158(2)	18(2)	12(2)			22.8	11.1		
	$5d6p\ ^1P_1$	52158(2)	18(2)	16(2)	52159	17				
	$6s7p\ ^1P_1$	52158(2)	19(2)	23(2)	52158	10			52200	11
	$6s8p\ ^1P_1$	52158(2)	20(2)	-32.7(2)			21	16.4		
$6p7p\ ^1P_1$	$6s6p\ ^1P_1$	50383(2)	25(2)	-22(2)						
	$5d6p\ ^1P_1$	50383(2)	29(2)	-28(2)	50383	26				
	$6s7p\ ^1P_1$	50383(2)	28(2)	-36(2)	50382	25	40.5	14.4	50405	28
	$6s8p\ ^1P_1$	50383(2)	29(2)	-45(2)						
$6p7p\ ^3D_1$	$5d6p\ ^1P_1$	51114 (2)	38(2)	21 (2)	51113	17				
	$6s7p\ ^1P_1$	51115(2)	39(2)	28(2)	51113	25			51142	21
	$6s8p\ ^1P_1$	51112(2)	38(2)	-38(2)						

level respectively and q is the line profile index parameter which plays a significant role in the line shape of the resonance [18]:

$$q = \frac{\langle \phi | \tilde{D} | i \rangle}{\pi V_E^* \langle \psi_E | \tilde{D} | i \rangle}.$$

Here \tilde{D} is the dipole operator and $|i\rangle$ is the initial bound state whereas $|\phi\rangle$ and $|\psi_E\rangle$ represents the discrete autoionizing state and the unperturbed continuum state respectively. The profile index parameter ' q ' represents the ratio of the transition probabilities to a discrete state and the continuum. When $|q| \rightarrow \infty$ the transition probability into the discrete state is dominant and the line profile will be Lorentzian. A small ' q ' value indicates a small transition amplitude in the discrete state and the line profile will be asymmetric whereas, when $|q| \rightarrow 0$ then the transition probability into the discrete state is much smaller than that into the continuum resulting a transmission window. The profile parameter q strongly depends upon the selection of the intermediate state from the ground state to the final excited state whereas the width of the autoionizing resonance reflects the strength of the coupling between the discrete autoionizing resonance with the underlying continuum and does not depend upon the excitation sequence.

The solid line in Figure 2a is the least square fit of equation (1) to the experimental data. The best fit yields the resonance energy $E_r = 52158(2)$ cm⁻¹, the width of the autoionizing line $\Gamma = 18(2)$ cm⁻¹ and line profile parameter $q = 12(2)$.

In the next experiment, we have recorded the same $6p7p\ ^3P_1$ autoionizing resonance from the $5d6p\ ^1P_1$ intermediate state. The atoms were excited to the intermediate state using a dye laser charged with LDS 698 and pumped with the second harmonic (532 nm) of the Nd:YAG laser. The dye laser, tuned at 700.4 nm, was frequency doubled by a BBO crystal to get the UV at 350.2 nm. In the second step, the $6p7p\ ^3P_1$ autoionizing resonance was approached using the dye laser charged

with Stillbire-420 dye and pumped by the THG (355 nm) of the Nd:YAG laser. The first laser was kept fixed at 350.2 nm while the second laser was scanned in the energy region 23445 cm⁻¹ to 23796 cm⁻¹ and the corresponding term energy 52000 cm⁻¹ to 52350 cm⁻¹ to record the $6p7p\ ^3P_1$ autoionizing resonance. The corresponding spectrum is shown in Figure 2b. The Fano formula is fitted to the recorded spectrum to extract the resonance energy, the width of the profile and the line shape parameter. The extracted values of these parameters are $E_r = 52158(2)$ cm⁻¹, $\Gamma = 18(2)$ cm⁻¹ and $q = 16(2)$ respectively.

In the third experiment, the $6p7p\ ^3P_1$ autoionizing resonance was recorded using $6s7p\ ^1P_1$ as an intermediate state. This intermediate state was approached using the frequency-doubled output of the dye laser charged with Rhodamine-640 tuned at 614.4 nm. The excited atoms were promoted to the $6p7p\ ^3P_1$ autoionizing state using a dye laser charged with Coumarine-500 and pumped by the THG (355 nm). The ionization signal covering the energy region 52000 cm⁻¹ to 52350 cm⁻¹ along with the least square fit of equation (1) is shown in Figure 2c. The best fit yields the resonance energy $E_r = 52158(2)$ cm⁻¹, spectral line width of the resonance $\Gamma = 19(2)$ cm⁻¹ and the profile parameter $q = 23(2)$.

In the fourth experiment, we have recorded the same $6p7p\ ^3P_1$ autoionizing resonance via the $6s8p\ ^1P_1$ intermediate state. The intermediate state was populated using the frequency-doubled output of the dye laser charged with Rhodamine-590 fixed at 557.2 nm while the autoionizing resonance was approached using the dye laser charged with Rhodamine-640. The Fano formula is fitted to the experimental data points shown in Figure 2d and the Fano-parameters have been extracted. The resonance energy, line profile index and the width of the $6p7p\ ^3P_1$ autoionizing line approached from four different intermediate states are listed in Table 1 along with the previously reported parameters.

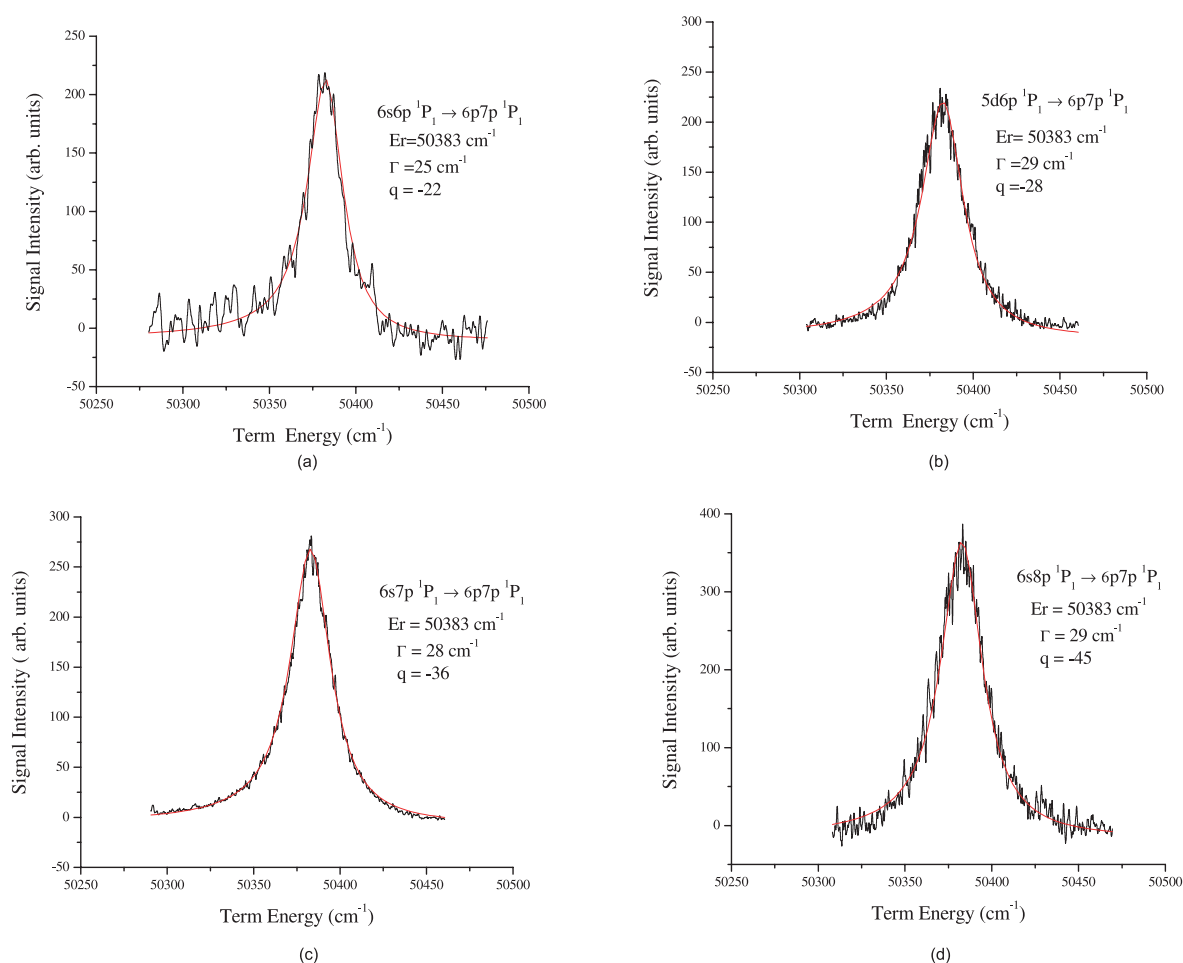
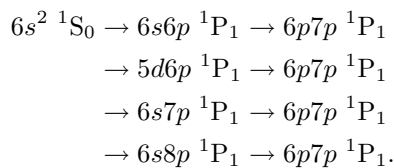


Fig. 3. The line shapes of the $6p7p \ ^1P_1$ autoionizing resonance of barium excited from (a) $6s6p \ ^1P_1$, (b) $5d6p \ ^1P_1$, (c) $6s7p \ ^1P_1$, (d) $6s8p \ ^1P_1$ the intermediate states. The solid line is the least square fit of equation (1).

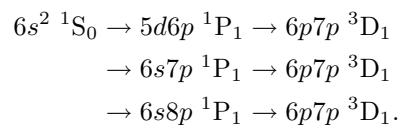
In the next series of experiments, we have studied the line profile of the $6p7p \ ^1P_1$ autoionizing resonance corresponding to the following transitions:



The intermediate states were acquired by tuning the first dye laser at 553.7 nm, 350.2 nm, 307.2 nm and 278.6 nm respectively while the second laser was scanned in the energy region from 32190 cm^{-1} to 32440 cm^{-1} , 21696 cm^{-1} to 21946 cm^{-1} , 17703 cm^{-1} to 17953 cm^{-1} and 14360 cm^{-1} to 14610 cm^{-1} respectively corresponding to term energy from 50250 cm^{-1} to 50500 cm^{-1} to record the $6p7p \ ^1P_1$ autoionizing resonance. In each case the resonance energy, line profile index and the width of the autoionizing resonance have been obtained from the least square fit of Fano formula (Eq. (1)) to the experimental spectral profiles. Figures 3a–3d shows the recorded experimental spectra corresponding to the above transitions respectively along with the least square fitted curves

of equation (1) to these data. The Fano parameters thus obtained are listed in Table 1.

In the third series of experiments, we have studied the line profile of the $6p7p \ ^3D_1$ autoionizing resonance corresponding to transitions:



The intermediate states $5d6p \ ^1P_1$, $6s7p \ ^1P_1$, $6s8p \ ^1P_1$ were populated by tuning the dye laser at 350.2 nm, 307.2 nm and 278.6 nm respectively while the ionizing laser was scanned in the specified energy region from 22446 cm^{-1} to 22696 cm^{-1} , 18453 cm^{-1} to 18703 cm^{-1} and 15110 cm^{-1} to 15360 cm^{-1} respectively corresponding to term energy 51000 cm^{-1} to 51250 cm^{-1} to record the $6p7p \ ^3D_1$ autoionizing resonance. From the photoionization spectra, we have extracted the resonance energy, line profile index and the width of the autoionizing resonance from the least square fitting of equation (1). The experimental spectra are shown in Figures 4a–4c respectively. The Fano parameters thus obtained are listed in Table 1.

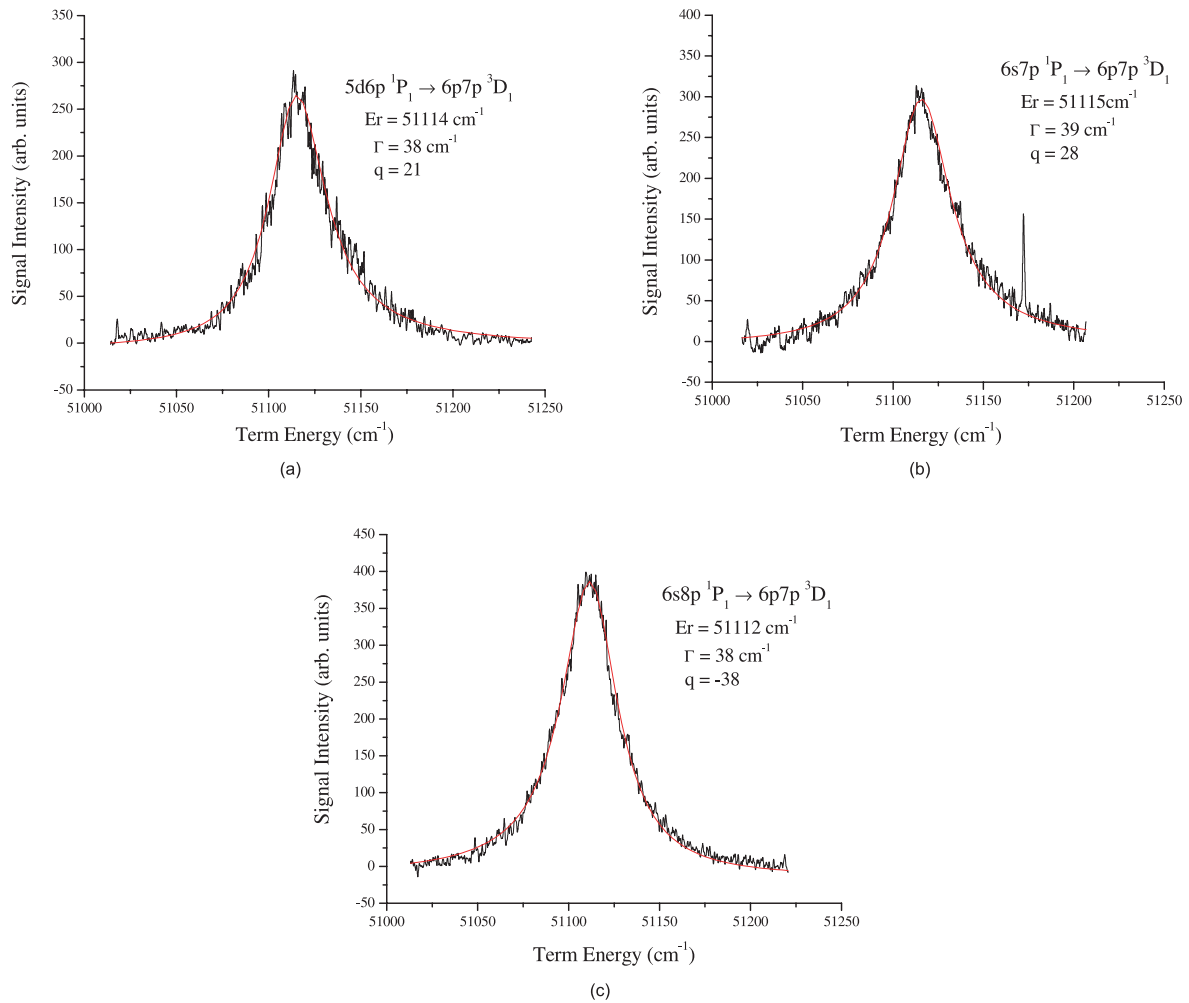


Fig. 4. The line shapes of the $6p7p\ ^3D_1$ autoionizing resonance of barium excited from (a) $5d6p\ ^1P_1$, (b) $6s7p\ ^1P_1$, (c) $6s8p\ ^1P_1$ the intermediate states. The smooth line is the Butler-Fano profile fitted to the experimental data.

The widths of the autoionizing resonances are determined by the strength of the mixed discrete states with the continuum states. If the interaction is caused by the operator of the electrostatic repulsion e^2/r_{ik} in LS-coupling, only the 1P_1 state of the mixed configuration $6p7p$ can interact with the continuum state $6s\epsilon p$ because of the selection rules with respect to the parity and other quantum numbers. The interaction $\langle 6s\epsilon p\ ^1P | e^2/r_{ik} | 6p7p\ ^1P \rangle$ is the strongest and the resulting signal exhibits a broad $6p7p\ ^1P_1$ resonance ($\Gamma \approx 28\text{ cm}^{-1}$) where as the interaction $\langle 6s\epsilon p\ ^1P | e^2/r_{ik} | 6p7p\ ^3P \rangle$ is much smaller and the autoionizing resonance is relatively narrower ($\Gamma \approx 19\text{ cm}^{-1}$) than the $6p7p\ ^1P_1$ resonance. Interestingly, the $6p7p\ ^3D_1$ resonance is the broadest ($\Gamma \approx 38\text{ cm}^{-1}$) among the observed resonances which, reflects a much stronger coupling with the continuum state.

The resonance energies of the $6p7p\ ^1P_1$, 3D_1 and 3P_1 autoionizing resonances determined in the present work are in good agreement with the experimental studies by Camus et al. [15] and Bobashev et al. [17] whereas the theoretical values by Luc-Koenig [19] are slightly higher than the experimental findings, the difference is less than

1 percent. Camus et al. [15] observed the $6p7p$ configuration based autoionizing resonance using the two-step optogalvonic detection technique and the widths of the autoionizing resonances were in the $17\text{--}26\text{ cm}^{-1}$ range while the widths of these resonances reported by Luc-Koenig et al. [19] based on the R -matrix and Multi-channel Quantum Defect Theory calculations were in the $11\text{--}28\text{ cm}^{-1}$ range. In the present work, the extracted values of the resonance widths ($18\text{--}38\text{ cm}^{-1}$) are slightly higher than that of the reported values. The larger width of the observed lines may be attributed to the depletion broadening or power broadening as described by Cooke et al. [24]. We have recorded the line profiles of these autoionizing lines at different ionizing laser intensities and observed that the width of the lines increases as a function of increased laser intensity. However, the profiles presented in this paper were recorded at much lower intensities and the profiles are power independent.

In Figure 5 the variation of the line widths of the $6p7p\ ^1P_1$, 3D_1 and 3P_1 autoionizing resonances and the term energy of the intermediate levels is presented. The dots are the experimentally observed data points with 10% error

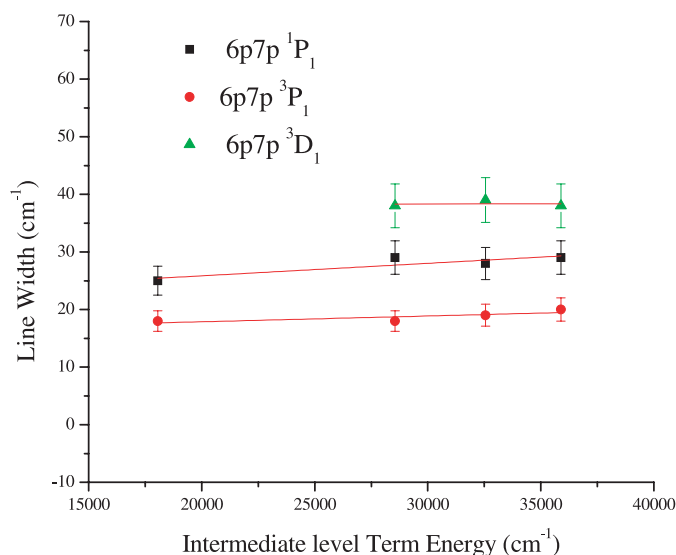


Fig. 5. Line width of the $6p7p$ 1P_1 , 3D_1 and 3P_1 autoionizing resonances versus the intermediate level term energy.

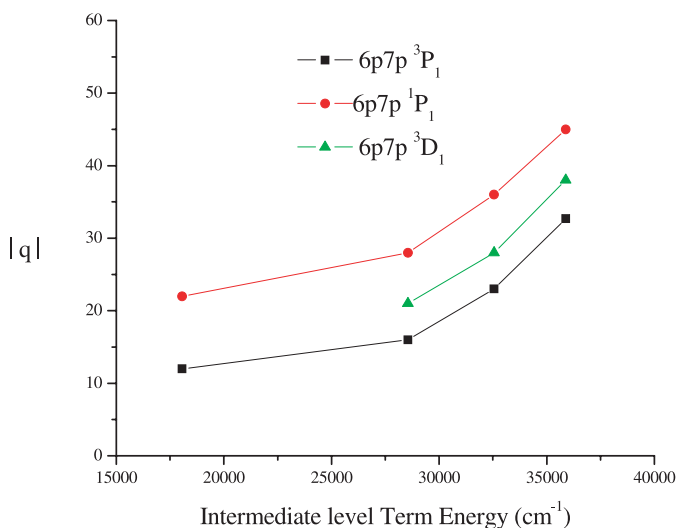


Fig. 6. Variation of the line profile parameter q of the $6p7p$ 3D_1 , 1P_1 and 3P_1 autoionizing resonances as a function of the intermediate level term energy.

bars and the solid lines are the linear regression fitting to these experimental data points. This figure manifests very beautifully the fact that the line widths remain constant with the change of the intermediate state and is independent of the excitation path.

Figure 6 represents the variation of the absolute value of the line profile parameter q versus intermediate level term energies. From the figure, it is evident that the $|q|$ increases with the increase in the term energies of the intermediate state. The larger value of the line profile parameter q indicates a symmetric Lorentzian line profile while a smaller value of q exhibits an asymmetric type resonance. The larger q -value corresponds to a stronger coupling between the bound intermediate state and the autoionizing state and a smaller q -value corresponds to

a weaker coupling between the bound intermediate state and the autoionizing state. This means, when we approach a specific autoionizing line via a lower bound intermediate state, then the coupling between the intermediate state and the autoionizing resonance is weaker and the q has a smaller value. When we achieve the same autoionizing state via other intermediate level lying above the first intermediate state, the coupling between the autoionizing resonance and the intermediate state is enhanced, thus q gets larger value. The stronger coupling between the intermediate and the autoionizing state corresponds to a dominant contribution of the autoionizing channel than direct ionization to the continuum and q has a larger value. On the other hand if the coupling between the intermediate and the autoionizing state is weaker, then the contribution of direct ionization channel becomes dominant than the autoionizing channel and the value of q decreases. In the present observations, the values of q are neither too large nor too small; these are in the range 12–45; which reflects that both the channels contribute in these transitions.

In conclusion we have recorded the $6p7p$ 1P_1 , 3D_1 and 3P_1 autoionizing resonances from different intermediate states. It is observed that the width of the autoionizing resonances does not depend on the excitation channel and it remains constant. It is further noticed that the line profile index parameter q depends on the excitation channels; its value enhances significantly as the intermediate states of higher term values are involved in the first step excitation.

The present work was financially supported by the Higher Education Commission (HEC), Pakistan Science Foundation (PSF-127), ICTP, Trieste, Italy under the ICAC affiliated centre scheme and the Quaid-i-Azam University, Islamabad, Pakistan. M.A. Kalyar, Sami-ul-Haq and Nasir Amin are grateful to the HEC for the grant of Ph.D. scholarship under the Indigenous scheme.

References

1. V.S. Letokhov, *Laser Photoionization Spectroscopy* (Academic Press, Florida, 1987)
2. T.F. Gallagher, *Rydberg Atoms* (Cambridge University Press, Cambridge, 1994)
3. W. Demtroder, *Laser Spectroscopy* (Springer, Berlin, 1996)
4. J.P. Connerade, *Highly Excited Atoms* (Cambridge University Press, UK, 1998)
5. J. Berkowitz, *Atomic and Molecular Photoabsorption* (Academic Press, New York, 2002)
6. J. Ganz, M. Raab, H. Hotop, J. Geiger, *Phys. Rev. Lett.* **53**, 1547 (1984)
7. J.S. Keller, J.E. Hunter III, R.S. Berry, *Phys. Rev. A* **43**, 2270 (1991)
8. M.A. Baig, M. Yaseen, Raheel Ali, Ali Nadeem, S.A. Bhatti, *Chem. Phys. Lett.* **296**, 403 (1998)
9. M. Stellpflug, M. Johnsson, I.D. Petrov, T. Halfmann, *Eur. Phys. J. D* **23**, 35 (2003)
10. J.J. Wynne, J.P. Hermann, *Opt. Lett.* **4**, 106 (1979)

11. R.R. Jones, T.F. Gallagher, *Phys. Rev. A* **38**, 2846 (1988)
12. M. Abutaleb, R.J. de Graaff, W. Ubachs, W. Hogervorst, M. Aymar, *J. Phys. B: At. Mol. Opt. Phys.* **24**, 3565 (1991)
13. Xiao Wang, W.E. Cooke, *Phys. Rev. A* **47**, 1778 (1993)
14. G. Waligorski, Lei Zhou, W.E. Cooke, *Phys. Rev. A* **55**, 1544 (1997)
15. P. Camus, M. Dieulin, A.El. Himdy, M. Aymar, *Phys. Scripta* **27**, 125 (1983)
16. A.Yu. Elizarov, N.A. Cherepkov, *Sov. Phys. JEPT* **69**, 4 (1989)
17. S.V. Bobashev, A. Yu. Elizarov, V.V. Korshunov, *Opt. Spectrosc.* **78**, 637 (1995)
18. U. Fano, *Phys. Rev.* **124**, 1866 (1961)
19. E. Luc-Koenig, M. Aymar, M. Millet, J.M. Lecomte, A. Lyras, *Eur. Phys. J. D* **10**, 205 (2000)
20. N. Amin, S. Mahmood, M. Anwar-ul-Haq, M. Riaz, M.A. Baig, *Eur. Phys. J. D* **37**, 23 (2006)
21. Sami-ul-Haq, S. Mahmood, N. Amin, Y. Jamil, R. Ali, M.A. Baig, *J. Phys. B: At. Mol. Opt. Phys.* **39**, 1587 (2006)
22. D. Hanna, P. Karkainen, R. Wyatt, *Opt. Quant. Electron.* **7**, 115 (1975)
23. C.E. Moore, *Atomic Energy Levels*, NSRDS-NBS, vol. III (Washington, DC, 1971)
24. W.E. Cooke, S.A. Bhatti, C.L. Cromer, *Opt. Lett.* **7**, 69 (1982)